CHAPTER VI

NOVEL CHITOSAN-SPOTTED ALGINATE FIBERS FROM WET-SPINNING OF ALGINATE SOLUTIONS CONTAINING EMULSIFIED CHITOSAN-CITRATE COMPLEX AND THEIR CHARACTERIZATION

6.1 Abstract

The major problem associated with the production of alginate/chitosan hybridized fibers by wet spinning is the formation of gels due to ionic interactions of the oppositely-charged molecules of alginate and chitosan when these two polymers are directly mixed. Here, we proposed a novel method of using chitosan in the form of an emulsion. Such an emulsion was prepared by adding the primary emulsion of olive oil in a sodium dodecyl sulphate (SDS) aqueous solution into chitosan-citrate complex. The complexation of chitosan with citric acid is the key of this method. The citrate ions neutralize the positive charges of chitosan, rendering the chitosan-citrate complex to be able to penetrate into the core of the SDS/olive oil micelles. The obtained emulsified chitosan-citrate complex (hereafter, the chitosan-citrate emulsion) of varying amount was then added into an alginate aqueous solution to prepare the alginate/chitosan spinning dope suspensions. The alginate/chitosan hybridized fibers showed spotty features of the chitosan-citrate complex micelles on the surface and the inside of the hybridized fibers. At the lowest content of incorporated chitosan (i.e., 0.5% w/w chitosan), both the tenacity and the elongation at break of the obtained chitosan-spotted alginate fibers were the greatest. Further increase in the chitosan content resulted in a monotonous decrease in the property values. Lastly, preliminary studies demonstrated that the obtained chitosan-spotted alginate fibers showed great promises as carriers for drug delivery.

(Key-words: Wet spinning; Alginate; Chitosan; Emulsion)

6.2 Introduction

Alginate and chitosan, polysaccharide biopolymers, have been the focal point of an expanding number of studies that address their potential for use in biomedical applications such as cell encapsulation (Iyer *et al.*, 2005; Krasaekoopt *et al.*, 2006), drug delivery (Tozaki *et al.*, 1999; Giunchedia *et al.*, 2002; Hejazi and Amiji, 2003), and tissue engineering (Pariente *et al.*, 2001). Alginate is a natural biopolymer obtained from cell walls of brown algae (Phaeophyta) such as the seaweeds *Laminaria* sp. and *Ascophyllum* sp. (Clare, 1993). It is a linear block copolymer consisting of uronic acid residues, namely β-D-mannuronic and α-L-guluronic acid, linked by (1→4)-linkages. Alginate-based products are popular for wound management, since they offer many advantages, e.g., biocompatibility, haemostatic capability, and gel-forming ability upon absorption of wound exudates (Jarvis *et al.*, 1987). Such gels prevent the wound bed from drying out, as a moist wound environment has been known to promote healing, leading to a better cosmetic repair of the wounds (Winter, 1962). Alginate is water-soluble and, in the presence of divalent cations, e.g., Ca^{2+}, alginate gels can be formed due to ionic cross-linking via calcium bridges between *L*-guluronic acid residues on adjacent chains (McDowell, 1974). Because of this reversible solubility, alginate can be fabricated in various forms (Agren, 1996; Dong *et al.*, 2006; Li *et al.*, 2005), resulting in the alginate-based dressings being made available as gel mats (e.g., AlgiSite®, Kaltostat®, and Tegagel®) (Paul and Sharma, 2004) and fiber mats (e.g., Algosteril®, Kaltostat®, and Sorbsan®) (Agren, 1996). Despite this, alginate itself does not possess an antimicrobial property and wounds often provide favorable environments for colonization of microorganisms, which may lead to infection and delay healing.

Chitosan, on the other hand, is a natural nontoxic biopolymer, derived from deacetylation of chitin, a major component of shells of crustaceans, such as crabs, shrimps, and crawfish. It has received considerable attention for its commercial applications in biomedical, food, and chemical industries (Knorr, 1984; Muzzarelli, 1977). Chitosan and chitosan oligomers have attracted considerable interest due to their biological activities, e.g., antimicrobial (Kendra and Hadwiger, 1984; Sekiguchi

et al., 1994; Sudarshan *et al.*, 1992), antitumor (Suzuki *et al.*, 1986; Tokoro *et al.*, 1988), and hypocholesterolemic functions (Sugano *et al.*, 1992). Ueno *et al.* (1999) reported that chitosan could promote wound healing in dogs, as it was observed to accelerate the infiltration of inflammatory cells, activate the migration of fibroblasts, and stimulate their proliferation in the wound area. Although chitosan can be produced in various forms, e.g., powder, films, beads, fibers and fabrics (Qin and Agboh, 1998; Qin *et al.*, 1997), products made from pure chitosan fibers have not been commercially viable, due to the poor tensile properties and the associated high processing costs. Moreover, the availability of chitosan in purified form is currently insufficient for a large-scaled production of the corresponding fibers. Poor solubility of chitosan in water also contributes to its limited applicability as a polysaccharide drug. This can be alleviated by chemical modifications (Kurita, 1998; Nishimura *et al.*, 1998); though the reaction course is often complicated and the isolation of products is usually prohibitive for a large-scaled production.

Combination of alginate and chitosan can compliment each other in the properties of the final products. One additional factor enabling the development of tailored biomaterials based on the use of both alginate and chitosan is through their potential to form a polyelectrolyte complex via ionic interactions. It is assumed that the carboxylate moieties on alginate molecules will ionically interact with the protonated amino groups on chitosan counterparts to form a three-dimensional matrix, known as a physically cross-linked hydrogel. Because of these opposite charges, a direct mixing of alginate and chitosan solutions would readily coagulate or form gels, leading to unfeasibility in the production of the respective alginate/chitosan fibers from mixed dope solutions of the polymers. Problems in the direct production of alginate/chitosan fibers can be overcome by several means. Some examples are the blending of separately fabricated alginate and chitosan fibers; the utilization of chitosan cationic core for the production of an alginate fiber (Cole and Nelson, 1993); and the coating of chitosan on calcium alginate filament (Tamura *et al.*, 2002). The latter is limited by the high molecular weight of chitosan, hence low concentrations of chitosan must be used to prevent the precipitation in the presence of the calcium ions (Tamura *et al.*, 2002). Knill *et al.* (2004) showed that the use of hydrolyzed chitosan for absorption into/coating onto an alginate filament

core could result in higher levels of chitosan incorporation, due to the greater mobility of the hydrolyzed chitosan chains. Notwithstanding, the majority of these methods have been based on the principle of coating via ionic interactions.

Here, we report a novel method for preparing alginate/chitosan hybridized fibers by wet-spinning a dope suspension prepared from direct mixing of an alginate solution and an emulsified chitosan suspension. Briefly, the alginate solution and the emulsified chitosan suspension were individually prepared and the emulsified chitosan suspension was subsequently added into the alginate solution under a vigorous stirring to obtain a homogeneous alginate/chitosan dope suspension. As distinguished from other previous methods, the method described here has the advantage of homogenizing the target substances prior to processing, thus homogeneity and composition of the substances can be controlled. Additionally, it is certain that all of the constituents in the dope suspension remain in the fibers and this method is convenient and easy to scale-up for a large-scaled production. The overall aims of this investigation were therefore (1) to develop a new method to maximize the chitosan content (so as to provide sufficient, beneficial properties of chitosan) by simply avoiding the direct interaction between alginate and chitosan through the use of the emulsified chitosan suspension, whilst retaining the textile-processing ability of alginate and (2) to investigate distinguished/outstanding properties of the obtained alginate/chitosan hybridized fibers thereby obtained.

6.3 Experimental

6.3.1 Materials

Chitosan flakes from crab shells (M_w = 40,000 Da) was kindly provided by Fujibo Co., Ltd. (Japan). Sodium alginate (viscosity of 10 g/L aqueous solution @ 20°C = 80~120 cP and pH of the same solution @ 25°C = 6~8), olive oil, sodium dodecyl sulfate (95.0% purity), anhydrous citric acid (98.0% purity), calcium chloride dihidrate ($CaCl_2.2H_2O$), Amido Black 10B, sodium hydroxide pellet (NaOH; 96.0% purity), acetic acid (99.9% purity), and methanol (MeOH; 99.7% purity) were purchased from Wako Pure Chemical Industries Co., Ltd. (Osaka, Japan).

6.3.2 Methods

6.3.2.1 Preparation of Chitosan Gel

Ten grams of chitosan flakes were first suspended in 1000 mL of distilled water under vigorous stirring (13200 rpm for 20 s). Twenty milliliters of acetic acid were subsequently added into the chitosan aqueous suspension under vigorous stirring (13200 rpm for 1 min) to obtain a clear chitosan aqueous solution. 10% NaOH aqueous solution was then added to adjust the pH of the chitosan aqueous solution under vigorous stirring (13200 rpm for 1 min). When the pH of the solution reached ~10-12, a clear chitosan gel was formed. The gel was further dialyzed in distilled water at room temperature to remove the residual NaOH until a neutral pH was obtained. Separation of the chitosan gel from the aqueous medium was carried out by centrifugation at 10000 rpm. The obtained chitosan gel was kept refrigerated prior to further use.

6.3.2.2 Preparation of Chitosan Emulsion

Two kinds of solutions were separately prepared. (1) *Chitosan solution* was prepared by adding citric acid powder into the as-prepared chitosan gel (the weight ratio of the chitosan gel in its dry state to citric acid was 1:1, equivalent to the mole ratio of ~0.84) under vigorous stirring until the chitosan gel dissolved completely (pH of the obtained chitosan solution was ~4). (2) *O/w emulsion* was prepared by homogenizing olive oil and 1% w/v sodium dodecyl sulphate (SDS) aqueous solution (the volume ratio of olive oil to the SDS solution = 6:4) under vigorous stirring (10600 rpm for 2 min), with this emulsion being referred to as "primary emulsion". The primary emulsion was then added drop-wise into the chitosan solution under vigorous stirring. The ratio of chitosan in the chitosan solution to the volume of the primary emulsion was 1 g:10 mL. The system was kept vigorously stirred until the suspension became completely homogenized. The reaction temperature was maintained at room condition (i.e., 25 ± 3°C) throughout the preparation process. The emulsified chitosan-citrate complex suspension obtained is hereafter referred to as "chitosan-citrate emulsion".

6.3.2.3 Fabrication of Neat and Chitosan-Spotted Alginate Fibers

The dope solution for preparing the neat alginate fibers was 4% w/v sodium alginate aqueous solution, while the spinning dope suspensions for

preparing the chitosan-spotted alginate fibers had been prepared by adding the as-prepared chitosan-citrate emulsion drop-wise into the as-prepared 4% w/v alginate aqueous solution under vigorous stirring (13200 rpm for 20 min). The volumetric ratio of the chitosan-citrate emulsion to the sodium alginate solution was varied to obtain the spinning dope suspensions with the weight ratio of chitosan to alginate in the range of 0.5 to 10% (see Table 6.1).

Table 6.1 Compositions and stretching conditions used for the preparation of neat alginate and chitosan-spotted alginate yarns

Chitosan:Alginate (% w/w)	Alginate (g)	Water (mL)	Chitosan gel[a] (g)	Citric acid (g)	Primary o/w[b] emulsion (ml)	Stretching unit speed (m/min)	
						DR1	DR2
0	4	100	-	-	-	5.9	7.2
0.5	4	100	0.57	0.02	2	5.9	7.2
1	4	100	1.14	0.04	4	5.9	7.2
2	4	100	2.29	0.08	8	5.9	7.2
4	4	100	4.57	0.16	16	5.9	7.2
10	4	100	11.43	0.4	40	8	9.7

[a] Weight of chitosan gel after back-calculation from the solid fraction of chitosan gel (solid fraction of chitosan from the obtained chitosan gel = 3.5% w/w).

[b] Volume ratio of olive oil to 1% w/v SDS aqueous solution = 6 : 4, the critical micelle concentration (CMC) in pure water at 25°C of SDS ~ 0.24% w/v.

The obtained solution/suspensions were homogeneous and stable. Prior to wet spinning, the as-prepared solution/suspensions were characterized for their viscosity as well as for the size of the emulsified chitosan particles (i.e., micelles) using a HAAKE RheoStress 600 Rheometer (at 25 °C) and an Olympus BX50 optical microscope, respectively. Note that the diameters of the chitosan-

citrate complex micelles were determined from representative microscopic images, from which ~100 particles were measured for their width and length using a SemAfore 4.0 image-analytical software.

Both the alginate solution and the alginate/chitosan suspensions had been left standing in the charging column at room temperature (i.e., 25 ± 3 °C) for degassing prior to being extruded through a spinneret (30 holes, diameter of which was 0.03 mm) into the first coagulation bath containing 5% w/v $CaCl_2$ in 50% v/v MeOH aqueous solution and the second coagulation bath containing MeOH. MeOH was chosen due to its being a non-solvent for alginate, thus allowing beneficial stabilization to the obtained yarns of 30 individual fibers. The obtained yarns were then drawn between two sets of rollers with the speeds as shown in Table 6.1, leading to the draw ratio of ~1.2. Finally, they were collected on bobbins, extensively washed with MeOH for 24 h, and dried at room temperature (i.e., 25 ± 3°C).

6.3.3 Characterization of Neat and Chitosan-Spotted Alginate Fibers

Chemical integrity of the neat and the chitosan-spotted alginate fibers were investigated by a Perkin-Elmer SPECTRUM 2000 Fourier transformed-infrared spectroscope (FT-IR). About 2 mg of the fiber samples was cut into small pieces for the preparation of KBr discs and recorded with 4 scans at a resolution of 4 cm^{-1}. Surface morphology and diameters of the neat and the chitosan-spotted alginate fibers were examined by a FE-SEM JEOL JSM-6700 scanning electron microscope, operating at an accelerating voltage of 5 kV. Each fiber specimen was coated with a thin layer of platinum, using a JEOL JFC-1500 sputtering device, prior to observation under SEM. Diameters of the fibers were measured directly from SEM images and the average values were calculated from 20 specimens. Staining of the yarns was achieved by immersing dried yarns in 0.01% w/v Amido Black 10B aqueous solution for 8 h and repeatedly rinsed with distilled water to remove the excess dye on the yarn surface. The stained yarns were then observed under an Olympus BX50 optical microscope. Lastly, mechanical integrity in terms of tenacity and elongation at break of both the neat and the chitosan-spotted alginate fibers was

tested on an ORIENTEC STA-1150 RTC Universal testing machine. The load cell, the gauge length, and the displacement rate used were 50 N, 10 mm, and 10 mm·min^{-1}, respectively.

6.4 Results and Discussion

6.4.1 Preparation of Chitosan-Citrate Emulsion

Citric acid, a weak organic acid, is known to exist in a variety of fruits and vegetables, most notably citrus fruits. In biochemistry, it is important as an intermediate in the citric cycle and, therefore, occurs in the metabolism of almost all living things. Citric acid has the highest salting-out effect in the so-called Hofmeister's series (Rosenholm *et al.*, 1999). Briefly, the three carboxylate groups of citric acid could ionically interact with other chemicals; thus, citric acid could be used to change the surface characteristic of the chemicals. Additionally, citrate ions have a potential to compete with water molecules in binding on the surface of colloid particles, rendering their dehydrating capability. Consequently, citric acid in its ionic form, in addition to its ability to lower the surface charge of a substance, can shorten the distance between charged particles by electrostatic adsorption or elimination of bound water molecules on the particle surface.

Chitosan in the presence of an organic acid could readily form a chitosan-organic acid complex (Okuyama *et al.*, 1999). As a result, citric acid in its ionic form is expected to form a complex with chitosan, thus inducing the non-polar character to the resulting complex. Specifically, interactions between the negative charges of the carboxylate groups of citric acid and the positive charges of the protonated amino groups of chitosan lead to the formation of chitosan-citrate complex. It is expected that the chitosan-citrate complex could reduce the hydrophilicity of chitosan. The low *M*w chitosan (i.e., 40,000 Da) was chosen here to increase its potential to form a complex with the citrate ions. Unlike the polycationic chitosan, the rather hydrophobic chitosan-citrate complex should be able to penetrate into the interior, hydrophobic part of micelles of the primary emulsion. The proposed mechanisms for the formation of the chitosan-citrate complex and the emulsified chitosan-citrate complex are shown in Schemes 6.1 and 6.2, respectively.

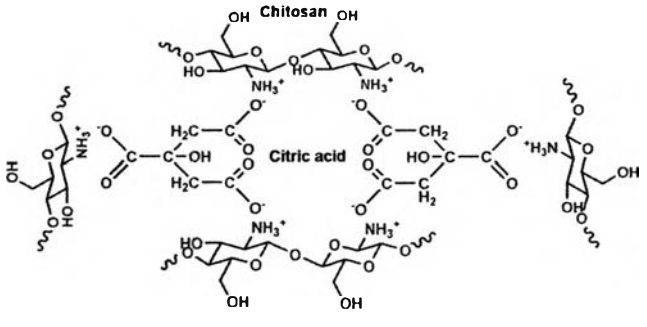

Scheme 6.1 Proposed mechanism for the formation of chitosan-citrate complex.

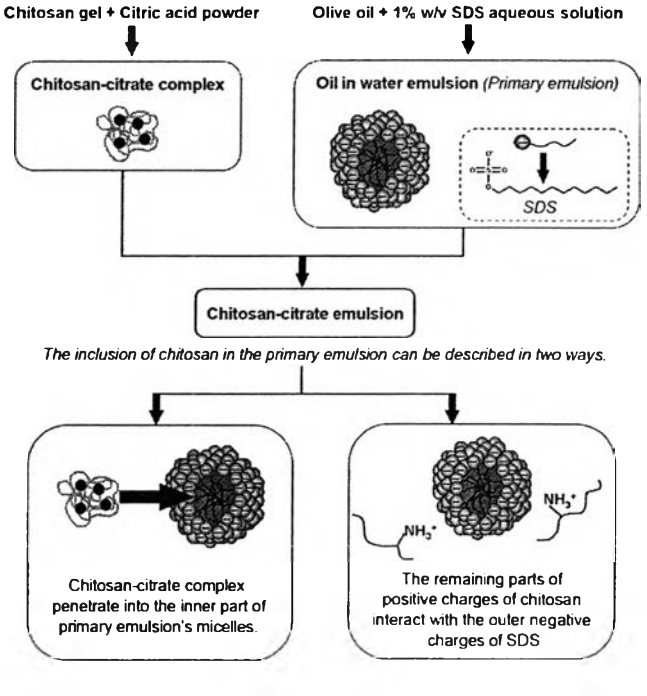

Scheme 6.2 Proposed mechanism for the formation of emulsified chitosan-citrate complex.

6.4.2 Microscopic Observation of Primary and Chitosan-Citrate Emulsions

The morphological appearance of the primary and the chitosan-citrate emulsions was examined using an optical microscope. Figure 6.1 shows representative microscopic images of the primary emulsion and the chitosan-citrate emulsion without and with the addition of the Amido Black 10B solution.

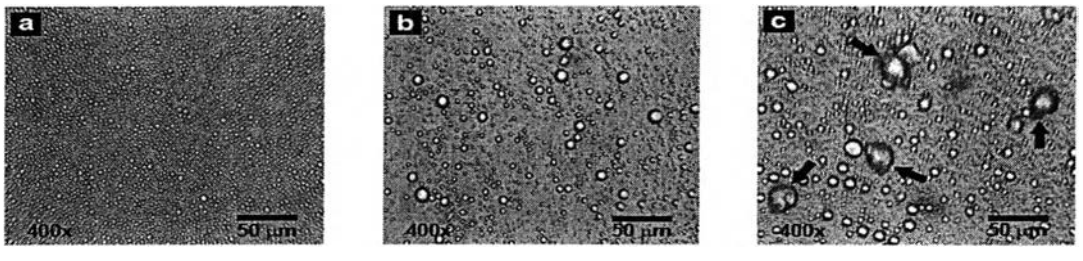

Figure 6.1 Microscopic images (magnification = 400x) of (a) o/w primary emulsion and chitosan-citrate emulsion (b) without and (c) with the addition of Amido Black 10B solution.

Transparent and spherical droplets of micelles are observed in all types of emulsions, with opaque droplets being additionally observed in the chitosan-citrate emulsion containing the dye. While the diameters of the droplets in the primary emulsion are relatively identical (i.e., 3.6 ± 0.9 μm), those of the droplets in the chitosan-citrate emulsion vary and are obviously greater than those of the droplets in the primary emulsion (i.e., 6.2 ± 2.0 μm). As with the chitosan-citrate emulsion containing the dye, the cationic, protonated amino groups of chitosan can form a complex with the anionic sulphate group of the anionic dye. Therefore, the droplets heavily-deposited with the dye, observed as the relatively-larger and darker droplets (see Figure 6.1c) in the chitosan-citrate emulsion, provide a clear evidence for the inclusion of chitosan in the form of the chitosan-citrate complex inside and/or the adsorption of it at the interface of the micelles in the chitosan-citrate emulsion. This confirms the proposed scheme illustrating the mechanism for the formation of the chitosan-citrate emulsion and reveals that the increase in the size of the micelles in the chitosan-citrate emulsion from that of the micelles in the primary emulsion is due to the inclusion of chitosan in the form of chitosan-citrate complex in the micelles.

6.4.3 Viscosity and Microscopic Observation of Neat Alginate Solution and Alginate/Chitosan Suspensions

Prior to the wet spinning, both the neat alginate solution and the alginate/chitosan suspensions were characterized for their shear viscosity and the size of the emulsified chitosan-citrate complex, and the results are summarized in Table 6.2.

Table 6.2 Shear viscosity of neat alginate solution and alginate/chitosan suspensions as well as size of the emulsified chitosan-citrate complex in the alginate/chitosan suspensions

Chitosan: Alginate (% w/w)	Apparent shear viscosity[a] (mPa s)	Size of emulsified chitosan-citrate complex[b] (μm)		Selected microscopic image of emulsified chitosan-citrate complex in an alginate/chitosan suspension[c]
		Width	Length	
0	1670 ± 82	-	-	
0.5	1602 ± 37	17.4 ± 7.8	31.4 ± 16.7	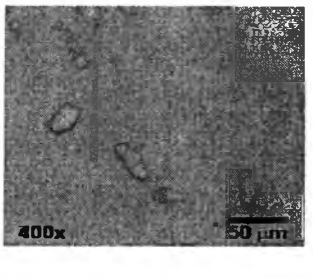
1	1604 ± 18	20.0 ± 7.6	39.0 ± 20.7	
2	1589 ± 30	25.2 ± 7.6	62.2 ± 22.9	
4	1559 ± 21	27.6 ± 10.2	82.5 ± 37.6	
10	1515 ± 44	25.0 ± 10.2	66.1 ± 30.6	

[a] At the apparent shear rate of 300 s^{-1} (n = 5).

[b] Measured from at least 100 particles.

[c] For the alginate/chitosan suspension containing 0.5% w/w chitosan (magnification = 400x).

The presence of the chitosan-citrate emulsion in the base alginate solution is responsible for the decrease in the apparent shear viscosity with an increase in the chitosan content. This should be due to the little to no specific

interactions between the alginate molecules and the chitosan-citrate complex micelles in the alginate/chitosan suspensions. As previously mentioned, the shape of the chitosan-citrate complex micelles in the chitosan-citrate emulsion was round. This is, however, not the case for such micelles in the alginate/chitosan suspensions. To illustrate the effect of the chitosan content on the size of the chitosan-citrate complex micelles, both the width and the length of the micelles were measured. According to Table 6.2, both quantities of the micelles increased from 17.4 ± 7.8 μm in width and 31.4 ± 16.7 μm in length for the alginate/chitosan suspension containing 0.5% w/w chitosan to reach maximal values at 27.6 ± 10.2 μm in width and 82.5 ± 37.6 μm in length for the suspension containing 4% w/w chitosan. Interestingly, at 10% w/w chitosan, both quantities of the micelles decreased to 25.0 ± 10.2 μm in width and 66.1 ± 30.6 μm in length. Evidently, the size of the micelles in the alginate/chitosan suspensions was significantly larger than that of the micelles observed in the chitosan-citrate emulsion. Drop coalescence could be the reason for the observed increase in the size of the micelles.

6.4.4 Chemical Integrity of Alginate/Chitosan Suspensions and Resulting Alginate Fibers

To investigate the chemical integrity of the individual ingredients in the alginate/chitosan suspensions and possible interaction among them, samples were analyzed by FT-IR spectroscopy. Figure 6.2 shows FT-IR spectra of (a) chitosan-citrate emulsion, (b) olive oil, (c) SDS and (d) chitosan gel, along with the chemical structures of the corresponding pure components. FT-IR spectra of chitosan display two strong vibrations at 1656 and 1595 cm^{-1}, corresponding to the vibrations of amide I and amide II, respectively (Osman and Arof, 2003; Smitha *et al.*, 2005). N-H and O-H stretchings of the carbohydrate ring are observed as a large band centering at 3430 cm^{-1}. Evidently, the majority of the band positions of the chitosan-citrate emulsion are identical to those of olive oil. Only the peak at 3467 cm^{-1} corresponding to the N-H and O-H stretchings of chitosan is noticeably different.

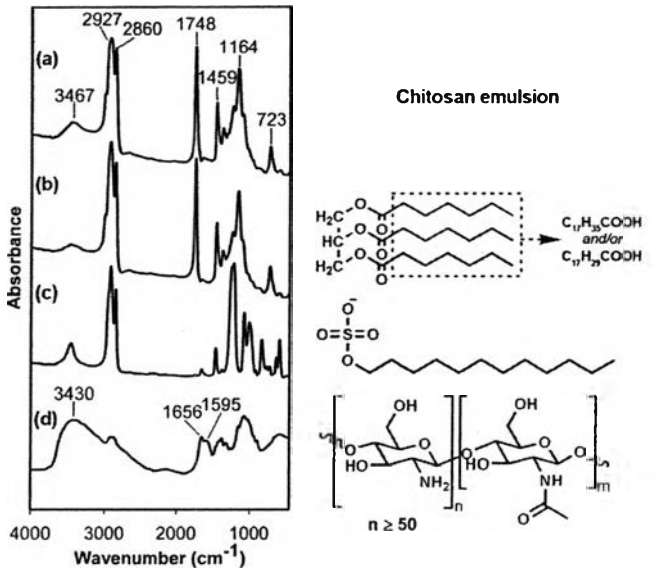

Figure 6.2 FT-IR spectra of (a) chitosan-citrate emulsion, (b) olive oil, (c) SDS and (d) chitosan gel, along with the chemical structures of the corresponding pure components.

FT-IR spectra of calcium alginate and chitosan-spotted alginate fibers are shown in Figure 6.3. Calcium alginate fiber display two vibrations that correspond to the carboxylate groups at 1623 cm^{-1} (antisymmetric stretching) and 1423 cm^{-1} (symmetric stretching). A peak belonging to the O-H stretching is also observed at 3437 cm^{-1}. The band positions are in agreement with those previously reported (van Hoogmoed *et al.*, 2007; Lawrie *et al.*, 2007). Clearly, the peaks corresponding to the $-COO^-$ and -OH functionalities are observed for all of the chitosan-spotted alginate fibers. Additional characteristic peaks of the chitosan-citrate emulsion at 2926 and 2852 cm^{-1} (C-H stretching), 1745 cm^{-1} (C=O stretching), 1164 cm^{-1} (C-O stretching of carboxylic acid and ester) and 717 cm^{-1} are observed. Intensities of these peaks increase with an increase in the chitosan content. This occurs simply as a consequence of a high local concentration of citric acid and olive oil associated with the presence of the chitosan-citrate emulsion in the fibers. Additionally, while the peak at 1623 cm^{-1} decreases in its intensity, the position of the peak at 1423 cm^{-1} shifts towards a higher wavenumber at ~1442-1457 cm^{-1}. This suggests possible interactions between alginate and chitosan-citrate emulsion, due to

the interactions between the free protonated amino groups ($-NH_3^+$) of chitosan and the carboxylate groups ($-COO^-$) of alginate.

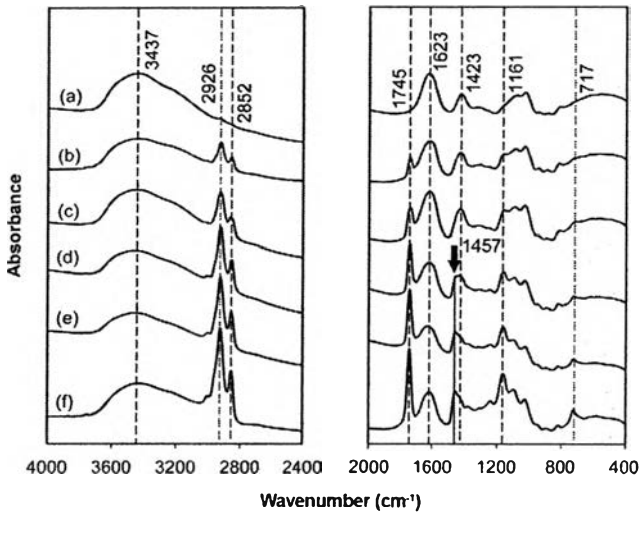

Figure 6.3 FT-IR spectra of (a) calcium alginate fiber and chitosan-spotted alginate fibers containing (b) 0.5, (c) 1, (d) 2, (e) 4, and (f) 10% w/w chitosan (base on the weight of alginate).

6.4.5 Effect of Chitosan Content on Morphology and Diameters of Resulting Alginate Fibers

Representative SEM micrographs of the calcium alginate and the chitosan-spotted alginate fibers are illustrated in Figure 6.4. Streak patterns can be visualized on the surface of the neat alginate fiber (see Figure 6.4A(a)). Both the roughness along the inner perimeter of each spinneret hole and the shrinkage upon drying of the fiber are postulated as the main reasons for the formation of these streaks. Streak patterns remains to be seen for the 0.5 and 1% w/w chitosan-spotted alginate fibers. As the chitosan content increases further, such streak patterns become less evident, with the occurrence of round protrusions or "spots" becoming discernible features on the surface of the fibers (see Figure 6.4A(b-f)). The occurrence of these spotty features should attribute to the presence of the chitosan-citrate complex micelles within the fibers. The size of the spots also increases with an increase in the chitosan content. Cross-sections of the 0.5 and 10% w/w chitosan-

spotted alginate fibers reveal that such spotty features also transcend to the inside of the fibers (see Figure 6.4B), though in a much less extent. During the extrusion of the alginate/chitosan spinning dope suspensions through the spinneret holes, there are great possibilities for the negatively-charged chitosan-citrate complex micelles to migrate to the boundary of the extrudate to interact with Ca^{2+} in the first coagulation bath. As a result, the spotty features tend to be at the fiber surface much more than at the inside of the fibers.

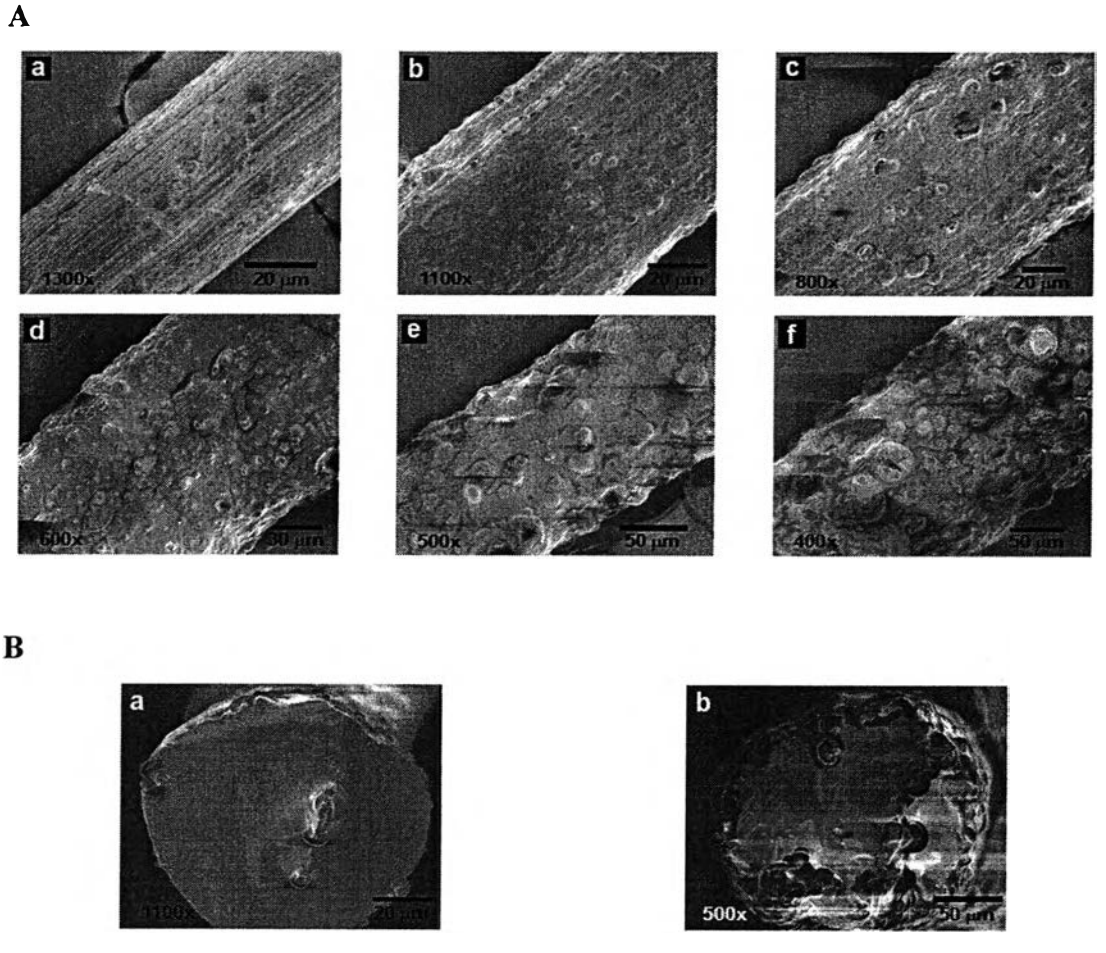

Figure 6.4 (A) Representative SEM images of (a) calcium alginate fiber and chitosan-spotted alginate fibers containing (b) 0.5, (c) 1, (d) 2, (e) 4, and (f) 10% w/w chitosan (base on the weight of alginate) and (B) cross-sectional SEM images of the chitosan-spotted alginate fibers containing (a) 0.5 and (b) 10% w/w chitosan.

As shown in Figure 6.5, the addition and increasing amount of chitosan in the neat alginate aqueous solution cause the diameters of the obtained fibers to increase from 51.4 ± 12.2 μm for the neat calcium alginate fiber to 192.4 ± 18.4 μm for the chitosan-spotted alginate fiber containing 10% w/w chitosan. The observed increase in the fiber diameters with the addition and increasing amount of chitosan in the form of the chitosan-citrate complex micelles should be due to the increase in both the number and the size of the micelles.

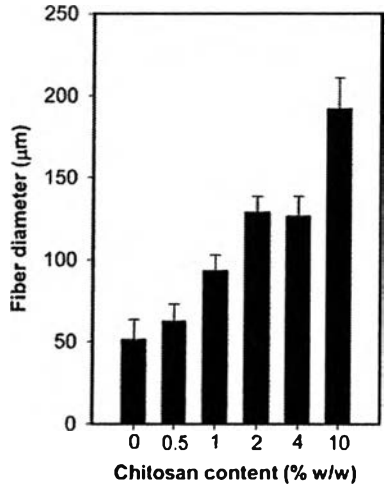

Figure 6.5 Diameters of calcium alginate and chitosan-spotted alginate fibers as a function of the chitosan content.

6.4.6 Distribution of Chitosan-Citrate Complex Micelles in Resulting Alginate Fibers

Similar to the result shown in Figure 6.1c, staining of the obtained chitosan-spotted alginate yarns with Amido Black 10B is a potent tool for examining the distribution of the chitosan-citrate complex micelles on the obtained fibers. Figure 6.6 shows representative microscopic images of the neat and the 10% w/w chitosan-spotted alginate yarns after having been immersed in 0.01% w/v Amido Black 10B aqueous solution for 8 h. While the neat alginate yarn shows negative staining for the dye, the opposite result was obtained with the 10% w/w chitosan-spotted alginate yarn. Figure 6.7 shows representative microscopic images of alginate fiber and chitosan-spotted alginate fibers containing 0.5-10% w/w chitosan

after staining. Similar to the result shown in Figure 6.6, no staining is observed on the neat alginate fiber. For the chitosan-spotted alginate fibers, the presence of the chitosan-citrate emulsion is evidenced from the occurrence of the stained spots. Clearly, both the diameter of the fibers and the number and the size of the spots are found to increase with an increase in the chitosan content.

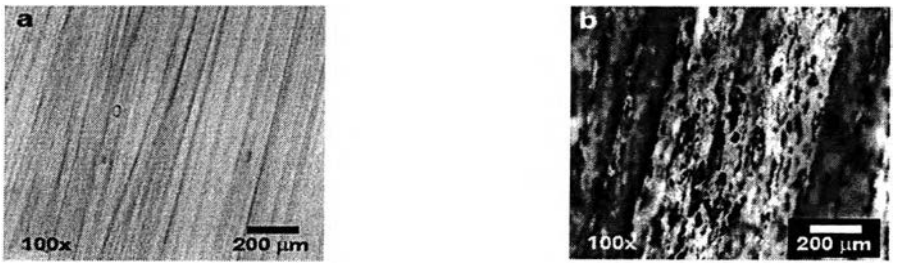

Figure 6.6 Representative microscopic images of (a) calcium alginate and (b) 10% w/w chitosan-spotted alginate yarns after immersion in 0.01% w/v Amido Black 10B aqueous solution for 8 h.

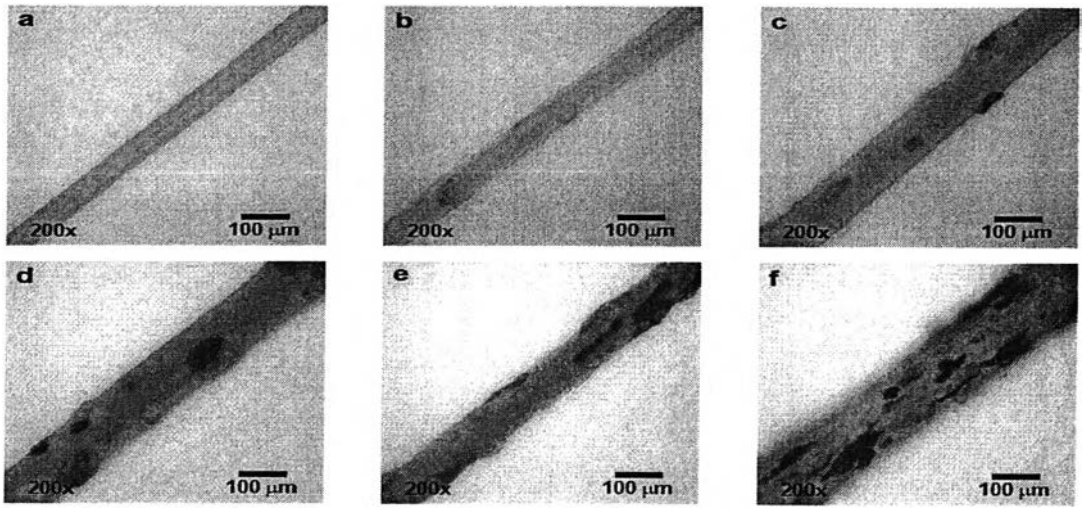

Figure 6.7 Representative microscopic images of (a) calcium alginate fiber and chitosan-spotted alginate fibers containing (b) 0.5, (c) 1, (d) 2, (e) 4, and (f) 10% w/w chitosan (base on the weight of alginate) after immersion in 0.01% w/v Amido Black 10B aqueous solution for 8 h.

6.4.7 Mechanical Integrity

Mechanical properties in terms of the tenacity and the elongation at break of both the neat and the chitosan-spotted alginate fibers were investigated and the results are shown in Figure 6.8. The tenacity of the neat alginate fibers is 4.3 ± 0.4 cN/tex, while the elongation at break is 20.4 ± 3.5%. The initial addition of the chitosan-citrate emulsion (i.e., at 0.5% w/w of chitosan) in the base alginate solution results in the observed increase in both the tenacity and the elongation at break from those of the neat alginate fibers. Further increase in the chitosan content from 1 to 10 % w/w results in the monotonous decrease in the property values of the obtained chitosan-spotted alginate fibers.

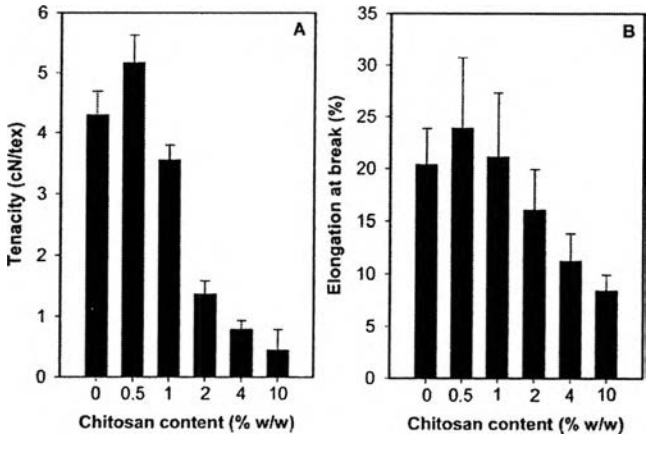

Figure 6.8 (A) Tenacity and (B) elongation at break of calcium alginate fibers and chitosan-spotted alginate fibers containing 0.5-10% w/w chitosan (based on the weight of alginate).

Based on both the SEM and the microscopic images shown in Figures 6.4 and 6.7, it is evident that the chitosan-spotted alginate fibers exhibit a character of a composite material (viz. the chitosan-citrate complex micelles behave as discrete entities within the alginate matrix). It is a known fact that mechanical properties of a composite depend not only on the amount, the size, the shape, and the alignment of the fillers, but also on the ability of the matrix to transfer the stress to the fillers (Sretenovic *et al.*, 2006). The latter depends solely on the interfacial affinity between

the matrix and the fillers. Even though FT-IR suggested that some interactions between the carboxylate groups of alginate and the protonated amino groups of chitosan do exist, the presence of chitosan in the form of the chitosan-citrate complex micelles should not contribute to the improvement in the rigidity of the obtained fibers, as the chitosan-citrate complex micelles are certainly not rigid entities. However, at 0.5% w/w of chitosan, both the tenacity and the elongation at break of the obtained fibers were the greatest. The reason for this could be due to the small amount of the chitosan-citrate complex micelles distributing within the fibers that does not cause a significant disruption to the continuity of the alginate matrix and, because of the weak interactions between the alginate and the chitosan chains previously mentioned, such mechanical properties could be enhanced.

6.4.8 Potential for Use of Chitosan-Spotted Alginate Fibers as Carriers for Drug Delivery

A preliminary, further investigation was carried out to explore the potential for use of the obtained chitosan-spotted alginate fibers as carries for drug delivery. Here, Amido Black 10B, an anionic dye, was used as a model anionic drug. In the first experiment, both the neat and the chitosan-spotted alginate fibers (2.5 cm in length for ~0.5 g) were immersed in 0.002% w/v Amido Black 10B aqueous solution for various time intervals in order to observe the kinetics of the dye adsorption. While a small amount of the dye could be adsorbed within the neat alginate fibers, a much larger amount of the dye could be adsorbed within the chitosan-spotted alginate fibers. Both the adsorption rate and the total of the adsorbed dye were found to increase with an increase in the chitosan content within the composite fibers. Furthermore, when the chitosan-spotted alginate fibers were submerged in phosphate buffer solution (pH 7.4) for 24 h, degradation of the fibers was observed, with the fibers that contained 4 and 10% w/w chitosan showing total disintegration of the fibers. These results demonstrate the feasibility of using the chitosan-spotted alginate fibers as carriers of anionic drugs. Detailed investigation concerning this will be further reported.

6.5 Conclusions

In the present contribution, gelation problem associated with the direct production of alginate/chitosan hybridized fibers has been overcome by the use of chitosan in the form of the chitosan-citrate emulsion. Microscopic images of the obtained chitosan-citrate emulsion demonstrated the successful inclusion of chitosan-citrate complex inside the micelles of the primary emulsion which had been prepared from olive oil and sodium dodecyl sulphate (SDS) aqueous solution. Varying amount of the chitosan-citrate emulsion was when mixed with the alginate aqueous solution to obtain the spinning dope suspensions for subsequent preparation into alginate/chitosan hydridized fibers by wet spinning. The maximum amount of chitosan was 10% w/w (based on the weight of alginate), which was significantly greater than previously-known methods. The obtained alginate/chitosan spinning dope suspensions were stable and homogeneous. SEM images clearly showed the occurrence of spotty features on the surface and the inside of the hybridized fibers. The number and the size of these spotty features as well as the diameters of the hydridized fibers increased with an increase in the chitosan content. Staining of the obtained hybridized fibers with Amido Black 10B, an anionic dye, confirmed that these spotty features were the chitosan-citrate complex micelles. Tensile properties in terms of tenacity and elongation at break were determined. At the lowest content of incorporated chitosan (i.e., 0.5% w/w chitosan), the number of the chitosan-citrate complex micelles within the obtained chitosan-spotted alginate fibers was not enough to disrupt the continuity of the alginate matrix. As a result, due to the weak interaction between alginate and chitosan molecules as suggested by FT-IR studies, both tensile property values were the greatest. However, as the chitosan content further increased, the property values were found to monotonically decrease, seemingly as a result of the increase in both the number and the size of the chitosan-citrate complex micelles. Lastly, preliminary studies demonstrated that the obtained chitosan-spotted alginate fibers showed great promises as carriers for drug delivery.

6.6 Acknowledgements

Financial support from 1) The Petroleum and Petrochemical College, Chulalongkorn University, 2) Kansai University, and 3) The Development and Promotion of Science and Technology Talent Project (DPST) is gratefully acknowledged.

6.7 References

Agren, M.S. (1996) Four alginate dressings in the treatment of partial thickness wounds: a comparative experimental study. British Journal of Plastic Surgery, 49(2), 129-134.

Clare, K. (1993) In R.L. Whistler, and J.N. BeMiller (Eds.), Industrial gums: Polysaccharides and their derivatives, San Diego: Academic Press, 105-143.

Cole, S.M., and Nelson, D.L. (1993) Alginate wound dressing of good integrity. US patent No. 5197945.

Dong, Z., Wang, Q., and Du, Y. (2006) Alginate/gelatin blend films and their properties for drug controlled release. Journal of Membrane Science, 280, 37-44.

Giunchedia, P., Julianoa, C., Gavinia, E., Cossua, M., and Sorrenti, M. (2002) Formulation and in vivo evaluation of chlorhexidine buccal tablets prepared using drug-loaded chitosan microspheres. European Journal of Pharmaceutics and Biopharmaceutics, 53, 233–239.

Hejazi, R., and Amiji, M. (2003) Chitosan-based gastrointestinal delivery systems. Journal of Controlled Release, 89, 151-165(15).

Iyer, C., Phillips, M., and Kailasapathy, K. (2005) Release studies of *Lactobacillus casei* strain Shirota from chitosan-coated alginate-starch microcapsules in *ex vivo* porcine gastrointestinal contents. Letters in Applied Microbiology, 41, 493-497.

Jarvis, P.M., Galvin, D.A.J., Blair, S.D., and McCollum, C.N. (1987) How does calcium alginate achieve hemostasis in surgery. Thrombosis and Haemostasis, 58(1), 80.

Kendra, D.F., and Hadwiger, L.A. (1984) Characterization of the smallest chitosan oligomer that is maximally antifungal to Fusarium solani and elicits pisatin formation in Pisum sativum. Fungal Genetics and Biology [Exp. Mycol.], 8(3), 276-281.

Knill, C.J., Kennedy, J.F., Mistry, J., Miraftab, M., Smart, G., Groocock, M.R., and Williams, H.J. (2004) Alginate fibres modified with unhydrolysed and hydrolysed chitosans for wound dressings. Carbohydrate Polymer, 55, 65-76.

Knorr, D. (1984) Uses of chitinous polymer in food-a challenge for food research and development. Food Technology, 38, 85-97.

Krasaekoopt, W., Bhandari, B., and Deeth, H.C. (2006) Survival of probiotics encapsulated in chitosan-coated alginate beads in yoghurt from UHT and conventionally treated milk during storage. LWT-Food Science and Technology, 39, 177–183.

Kurita, K., Shimada, K., Nishiyama, Y., Shimojoh, M., and Nishimura, S.I. (1998) Nonnatural branched polysaccharides: synthesis and properties of chitin and chitosan having α-mannoside branches. Macromolecules, 31(15), 4764-4769.

Lawrie, G., Keen, I., Drew, B., Temple, A.C., Rintoul, L., Fredericks, P., and Grøndahl, L. (2007) Interactions between Alginate and Chitosan Biopolymers Characterized Using FTIR and XPS. Biomacromolecules, 8(8), 2533-2541.

Li, Z., Ramay, H.R., Hauch, K.D., Xiao, D., and Zhang, M. (2005) Chitosan-alginate hybrid scaffolds for bone tissue engineering. Biomaterials, 26, 3919-3928.

McDowell, R.H. (1974) In Properties of Alginates, 3rd Ed. London: Alginate Industry Limited.

Muzzarelli, R.A.A. (1977) Chitin; Pergamon Press: Oxford.

Nishimura, S.I., Kai, H., Shinada, K., Yoshida, T., Tokura, S., Kurita, K., Nakashima, H., Yamamoto, N., and Uryu, T. (1998) Regioselective syntheses of sulfated polysaccharides: specific anti-HIV-1 activity of novel chitin sulfates. Carbohydrate Research, 306, 427-433.

Okuyama, K., Noguchi, K., Hanafusa, Y., Osawa, K., and Ogawa, K. (1999) Structural study of anhydrous tendon chitosan obtained via chitosan/acetic acid complex. International Journal of Biological Macromolecules, 26, 285-293.

Osman, Z., and Arof, A.K. (2003) FTIR studies of chitosan acetate based polymer electrolytes. Electrochimica Acta, 48, 993-999.

Pariente, J.L., Kim, B.S., and Atala, A. (2001) In vitro biocompatibility assessment of naturally derived and synthetic biomaterials using normal human urothelial cells. Journal of Biomedical Materials Research, 55(1), 33-39.

Paul, W., and Sharma, C.P. (2004) Chitosan and alginate wound dressings: a short review. Trends in Biomaterials and Artificial Organs, 18(1), 18-23.

Qin, Y., and Agboh, O.C. (1998) Chitin and chitosan fibres: unlocking their potential. Medical Device Technology, 9(10), 24-28.

Qin, Y., Agboh, O.C., Wang, X., and Gilding, D.K. (1997) Novel polysaccharide fibres for advanced wound dressings. In Medical textiles 96, S.C. Anand, Eds.; Cambridge: Woodhead Publishing Limited, pp. 15-20.

Rosenholm, J.B., Nylund, J., and Stenlund, B. (1999) Synthesis and characterization of cationized latexes in dilute suspensions. Colloids and Surfaces A: Physicochemical and Engineering Aspects, 159, 209-218.

Sekiguchi, S., Miura, Y., Kaneko, H., Nishimura, S.I., Nishi, N., Iwase, M., and Tokura, S. (1994) Molecular weight dependency of antimicrobial activity by chitosan oligomers. In Food Hydrocolloids: Structures, Properties, and Functions; Nishinari, K., and Doi, E., Eds., PlenumPress, New York, pp. 71-76.

Smitha, B., Sridhar, S., and Khan, A.A. (2005) Chitosan-sodium alginate polyion complexs as fuel cell membrane. European Polymer Journal, 41, 1859-1866.

Sretenovic, A., Muller, U., and Gindl, W. (2006) Mechanism of stress transfer in a single wood fiber-LDPE composite by means of electronic laser speckle interferometry. Composites Part A: applied science and manufacturing, 37, 1406-1412.

Sudarshan, N.R., Hoover, D.G., and Knorr, D. (1992) Antibacterial action of chitosan. Food Biotechnology, 6(3), 257-272.

Sugano, M., Yoshida, K., Hashimoto, M., Enomoto, K., and Hirano, S. (1992) In Advances in Chitin and Chitosan; Brine, C.J., Sandford, P.A., Zikakis, J.P., Eds.; Elsevier, London, pp. 472-478.

Suzuki, K., Mikami, T., Okawa, Y., Tokoro, A., Suzuki, S., and Suzuki, M. (1986) Antitumor effect of hexa-*N*-acetylchitohexaose and chitohexaose. Carbohydrate Research, 151, 403-408.

Tamura, H., Tsuruta, Y., and Tokura, S. (2002) Preparation of Chitosan-coated Alginate Filament. Material Science and Engineering, C20, 143-147.

Tokoro, A., Takewaki, N., Suzuki, K., Mikami, T., Suzuki, S., and Suzuki, M. (1988) Effect of hexa-*N*-acetylchitohexaose and chitohexaose aginst Meth-A solid form. Chemical & Pharmaceutical Bulletin, 36(2), pp. 784-790.

Tozaki, H., Fujita, T., Odoriba, T., Terabe, A., Okabe, S., Muranishi, S., and Yamamoto, A. (1999) Validation of a pharmacokinetic model of colon-specific drug delivery and the therapeutic effects of chitosan capsules containing 5-aminosalicylic acid on 2,4,6-trinitrobenzenesulphonic acid-induced colitis in rats. Journal of Pharmacy and Pharmacology, 51, 1107-1112.

Ueno, H., Yamada, H., Tanaka, I., Kaba, N., Matsuura, M., Okumura, M., Kadosawa, T., and Fujinaga, T. (1999) Accelerating effects of chitosan for healing at early phase of experimental open wound in dogs. Biomaterials, 20, 1407-1414.

van Hoogmoed, C.G., Busscher, H.J., and de Vos, P. (2003) Fourier transform infrared spectroscopy studies of alginate-PLL capsules with varying compositions. Journal of Biomedical Materials Research Part A, 67(1), 172-178.

Winter, G.D. (1962) Formation of the scab and the rate of epithelialization of superficial wounds in the skin of the young domestic pig. Nature, 193, 293-294.